JOURNAL OF MATERIALS SCIENCE **40** (2005) 5265–5268

Doppler broadening measurements of the electron-positron annihilation radiation in nanocrystalline ZrO_2

M. CHAKRABARTI
Department of Physics, University of Calcutta, 92 Acharya Prafulla Chandra Road, Kolkata 700009, India; Variable Energy Cyclotron Centre, 1/AF, Bidhannagar, Kolkata 700064, India

D. BHOWMICK
Variable Energy Cyclotron Centre, 1/AF, Bidhannagar, Kolkata 700064, India

A. SARKAR
Department of Physics, University of Calcutta, 92 Acharya Prafulla Chandra Road, Kolkata 700009, India; Department of Physics, Bangabasi Morning College, 19 Rajkumar Chakraborty Sarani, Kolkata 700 009, India

S. CHATTOPADHYAY
Department of Physics, University of Calcutta, 92 Acharya Prafulla Chandra Road, Kolkata 700009, India

S. DECHOUDHURY, D. SANYAL*, A. CHAKRABARTI
Variable Energy Cyclotron Centre, 1/AF, Bidhannagar, Kolkata 700064, India
E-mail: dirtha@veccal.ernet.in

ZrO_2 powders have been ground by ball mill grinder to achieve the particle size down to 10 nm. Typical defects introduced during ball mill grinding have been studied by positron annihilation lifetime measurement technique and coincidence Doppler broadened positron annihilation radiation spectroscopic technique. Coincidence Doppler broadened positron annihilation spectra for ball mill ground and unground ZrO_2 samples have been analyzed by constructing ratio curve with defects free Al single crystal. Results indicate an increase of cation defects in ZrO_2 samples due to the reduction of particle size by the ball mill grinding process.

1. Introduction

Materials in nanocrystalline phase become more interesting as the electrical, magnetic and optical properties change drastically due to the reduction of particle size [1–4]. Nanocrystalline ceramic oxides are of specially important because of their advanced mechanical properties. In these ceramic oxide systems, ZrO_2 is more interesting as it shows high strength [5], relatively high dielectric constant (∼25, compared to 3.5 for SiO_2), good thermal stability (when in direct contact with Si) and a wide band gap (5.1-7.8 eV) [6]. At room temperature the monoclinic phase of ZrO_2 is stable but due to doping of the Ca^{2+}, Mg^{2+} or Y^{3+} ions (<16 mol%) tetragonal phase stabilizes [7]. These stabilized zirconia alloys have interesting mechanical and ionic properties which make possible to use it as structural and wear components, oxygen gas sensors, fuel cells, etc., [8]. ZrO_2 has also been used as a suitable target material for the production of radioactive ions [9] in isotope separator on line radioactive ion beam facilities. Diffusion of the produced radioactive species from the target material (refractive materials e.g., Al_2O_3, ZrO_2 etc.) is very important for the production of high intensity radioactive ion beam. One can think of a nanocrystalline powder material for these purposes as both the volume diffusion and the interface diffusion have been enhanced significantly by reducing the particle size in addition to a faster release of the produced short-lived radioactive isotopes from the target material.

There are several methods for the preparation of the nanocrystalline oxides. These include the chemical vapor phase deposition method [10], gas condensation technique [11], sol-gel syntheses [12], oxidation of nanocrystalline materials [13], calcinations of hydroxides [14], radio frequency sputtering [15] and high energy ball milling process [16] etc. Among these processes high energy ball milling process has many potential advantages for the preparation of nanocrystalline

*Author to whom all correspondence should be addressed.
0022–2461
DOI: 10.1007/s10853-005-0743-3

samples [17]. The main advantage is, large quantities of samples have been produced in a very short time and the process is relatively simple and inexpensive.

During the preparation of nanocrystalline oxides by ball mill grinding large number of defects are introduced inside the material [18]. In the nanocrystalline phase the surface to volume ratio is very high, hence the surface defects play an important role in determining the optical and the electronic properties of the material. It is very important to study these defects also. One can employ positron annihilation technique, a well known nuclear solid state technique [19], to explore information about these defect sites. Presently we have used ball milling process to prepare the nanocrystalline ZrO_2 and employed positron annihilation technique to study these defects in different particle sized ZrO_2.

2. Experimental outline

2.1. Sample preparation

ZrO_2 powder (Aldrich Chem. Comp., 99.9% purity) has been milled in a commercial planetary (Fritsch Pulverisette 5) ball mill grinder for different periods to achieve lower particle size. 4 gm of powder was placed in a stainless steel vial of 80 ml volume charged with 12 stainless steel balls ($m_{\text{balls}} = 4$ gm) of 10 mm diameter for the purpose of milling. The ball to powder weight ratio was 12:1. The angular velocity of the supporting disc was kept at 300 rpm. The milling time was varied from 3 hour to 25 h.

2.2. Sample characterization by XRD and TEM

Average grain sizes of the ball milled ZrO_2 powder have been determined by X-ray diffraction (XRD) pattern. The X-ray diffraction data are collected on a Philips PW 1710 automatic diffractometer with Cu K_α tube operating at 40 kV and 20 mA in the 2θ range from 20° to 60° in a step size of 0.02°. The mean grain sizes, D, have been determined from the Scherrer equation [20]

$$D = K\lambda/(\beta \cos\theta)$$

where $K = 0.89$, β is the full width at half maximum height of a diffraction peak at an angle θ and λ is the wavelength of the Cu K_α radiation.

The transmission electron microscopy has been done with a 120 kV JEM-200CX Electron Microscope. A few droplets of powder, ultrasonically dispersed in alcohol, have been put on standard microscope grid for the TEM work. The sizes of about five grains at about four locations or bright field images (one such micrograph has been shown in Fig. 1) have been measured for each sample.

2.3. Positron annihilation studies

About 10 μCi ^{22}Na source enclosed between two thin (2 μm thick) nickel foils has been used as a positron source. The source has been sandwiched between two identical and plane faced pellets of ZrO_2. The positron annihilation lifetimes (PAL) have been measured with a fast-slow coincidence assembly having a time resolution of 190 ps [21]. Measured PAL spectra ($\sim 10^6$ coincidence counts) have been analyzed by computer programme PATFIT-88 [22] with necessary source corrections to evaluate the possible lifetime components τ_i, and their corresponding intensities I_i.

Coincidence Doppler broadening of the positron annihilation γ-radiation (CDBPAR) has been measured by an HPGe detector having energy resolution of 1.1 keV for the 514 keV line of ^{85}Sr. The two detector coincidence technique [23] has been used to achieve the higher peak to background ratio (14000:1) in the measured spectrum under the 511 keV photo-peak. A total of 2×10^6 coincidence counts have been recorded with a counts rate of 110 per second. The CDBPAR spectra for unground and ball mill ground samples have been analyzed by constructing the "ratio-curve" [24, 25] with defects free Al single crystal. The CDBPAR spectra at different nanocrystalline ZrO_2 samples have been also analyzed by constructing the "ratio-curve" with the unground sample.

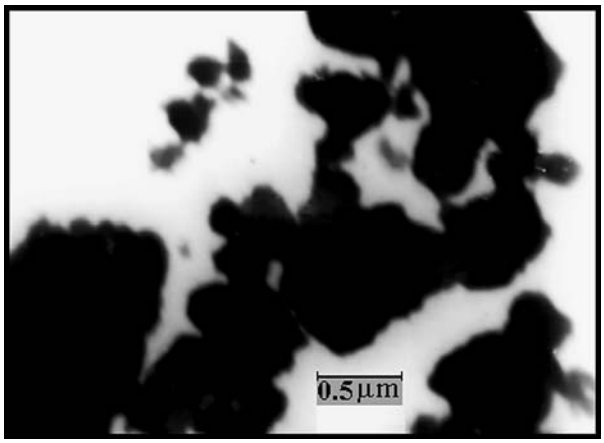

Figure 1 TEM image of the unground ZrO_2.

3. Results and discussion

The XRD patterns of the ball milled samples are shown in Fig. 2. From Fig. 2 it is clear that due to ball milling a major percentage of ZrO_2 becomes amorphous which

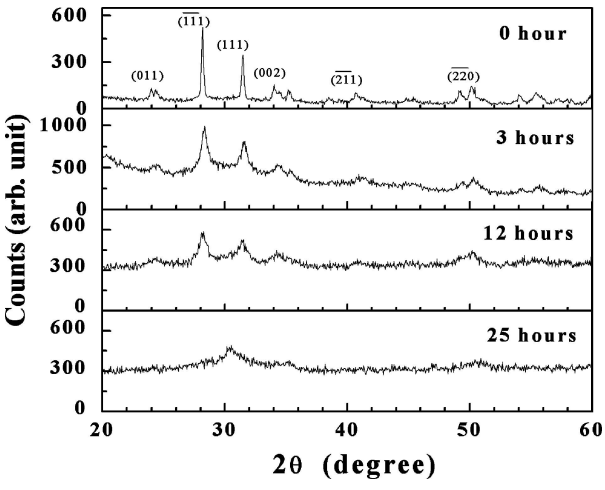

Figure 2 X-ray diffraction patterns of the unground and differently ball mill ground ZrO_2.

is in agreement with previous observations [7, 16]. The monoclinic phase of the sample is confirmed from Fig. 2. The particle sizes, as calculated from Scherrer equation at peak 28.16° (the $\bar{1}11$ reflection), are 222, 40, 26 and 8 nm for unground, 3, 12 and 25 h ball milled, respectively. The other prominent peak at 31.5° (111 reflection) corresponds to the 101 reflection of the tetragonal phase confirming a small amount of tetragonal phase present in our sample. The particle size obtained from TEM micrographs is of the order of 300 nm for the unground sample whereas this reduces to 50, 33 and 10 nm during 3, 12 and 25 h of ball milling. These particle sizes are in well agreement with those obtained from XRD analysis.

Each positron annihilation lifetime spectra have been fitted with one to three lifetime components fitting but the best fit (variance of fit $\leq$1 per channel) has been observed for three lifetime components fit. The fitted spectra results a very long lifetime component ($\tau_3 \sim$ 1.6 ns) present for all these samples with a very small intensity. This lifetime component is due to the formation of ortho positronium and its subsequent decay as para positronium (pick-off process) in large defect sites. The other two lifetime components are attributed to the free annihilation of positron ($\tau_1 \sim 117$ ps) and the annihilation of the positrons at the defect sites (τ_2, the intermediate lifetime component). τ_2 is considered to be the most significant positron annihilation lifetime parameter in the present system. The fraction of positrons annihilating at this particular defect sites is represented by I_2, the intensity of the intermediate lifetime component. Variations of τ_2 and I_2 with particle sizes are graphically shown in Fig. 3. Due to the reduction of particle sizes a small decreasing nature of τ_2 has been observed (as depicted in Fig. 3) but its relative intensity, I_2, increases largely. This suggest that the nature of this particular defect site remains almost unaltered only its number increases largely due to the reduction of particle size by ball mill grinding.

Fig. 4 represents the ratio-curve of the CDBPAR spectra for unground and ball mill ground ZrO_2 with the defects free Al single crystal. Fig. 4 shows a peak at $\sim 11 \times 10^{-3}$ m_0c and another broad peak in the momentum range ($20 < p_1 < 30$) $\times 10^{-3}$ m_0c. The peak at $\sim 11 \times 10^{-3}$ m_0c is due to the annihilation of positrons with the 4d electrons of the Zr atom [24] and the other broad flat peak ($p_1 > 20 \times 10^{-3}$ m_0c) is due to the annihilation of positrons with the 4p electrons of the Zr atom [24]. From Fig. 4 it is clear that although the nature of the ratio curve is almost same for both unground and ball mill ground ZrO_2 powder (12 and 25 h ball mill ground) but their peak heights are different. The peak height gradually decreases as the particle size decreases from ~300 nm (unground) to ~33 nm (12 h ball mill ground) and to ~10 nm (25 h ball mill ground). The gradual decrease of peak height suggests a gradual increase of defects introduced in ZrO_2 system [24] due to ball milling. To identify these defects we have constructed ratio curve for differently (3, 12 and 25 h) ground ZrO_2 with the unground ZrO_2. Fig. 5 represents the ratio curves of the ball-mill ground ZrO_2 (nanocrystalline) with the unground ZrO_2. Each of the ratio curves (Fig. 5) has two dips, one dip at around (13-17) $\times 10^{-3}$ m_0c and another sharp dip at 27×10^{-3} m_0c. This clearly indicates that in case of ball mill ground ZrO_2 (nanocrystalline ZrO_2) positrons are less annihilating with the 4d (first dip) as well as 4p (second dip) electrons of the Zr atom. Less annihilation of positrons with the electrons at the Zr site confirms the presence of cation defects in this system.

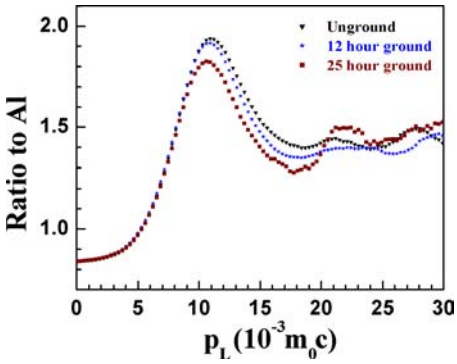

Figure 4 Ratio of the experimental electron-positron momentum distributions for the unground ZrO_2 and the ball mill ground (nanocrystalline) ZrO_2 to the electron-positron momentum distributions for the defects free Al single crystal.

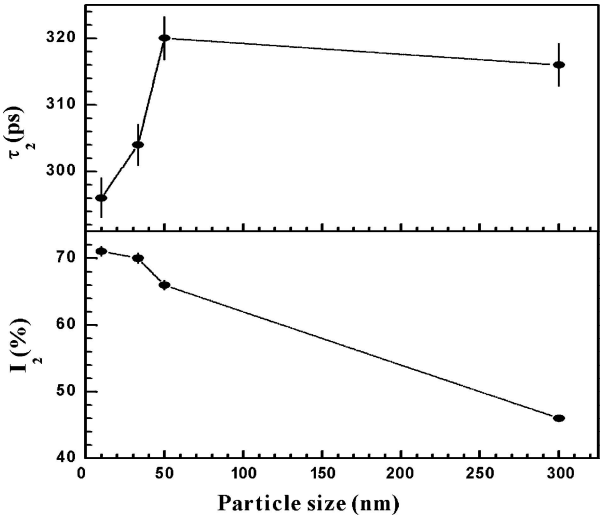

Figure 3 Variations of τ_2 and I_2 with different particle size of the ZrO_2.

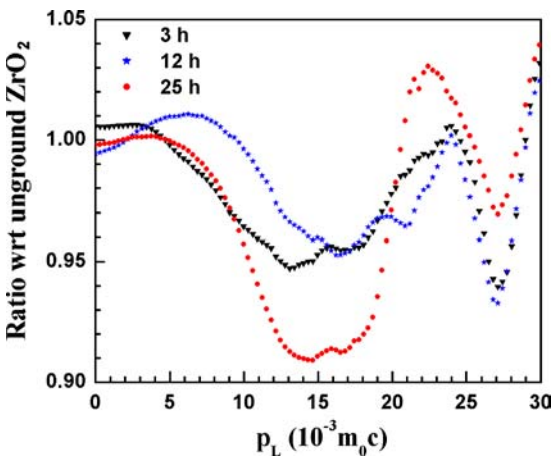

Figure 5 Ratio of the experimental electron-positron momentum distributions for the ball mill ground (nanocrystalline) ZrO_2 to the electron-positron momentum distributions for the unground ZrO_2.

Thus the CDBPAR data analysis indicates that due to the reduction of particle size by ball mill grinding process cation defects are introduced in the ZrO_2 system similar to CuO [26] and the drastic change of I_2 (from 46 to 70%) with the particle size (Fig. 3) is also due to the increase of these cation defects in the ZrO_2 system.

4. Conclusion

Ball milled ZrO_2 powders (particle size down to 10 nm) have been characterized by powder X-ray diffraction method. Analysis of the CDBPAR spectra and the positron annihilation lifetime spectra for differently ball mill ground ZrO_2 powder indicate an increase of cation defects in ZrO_2 samples due to the reduction of particle size.

Acknowledgement

One of the authors (S.C) gratefully acknowledges the CSIR, New Delhi for providing financial assistance.

References

1. R. NITSCHE, M. WINTERER, M. CROFT and H. HAHN, *Nucl. Instr. Meth.* B **97** (1995) 127.
2. R. W. SEIGEL and G. E. FOUGERE, *Nanostruct. Mater.* **6** (1995) 205.
3. H. GLEITER, *Acta Mater.* **48** (2000) 1.
4. H. HAHN and R. S. AVERBACK, *J. Am. Ceram. Soc.* **74** (1991) 2918.
5. R. H. J. HANNINK, P. M. KELLY and B. C. MUDDLE, *ibid.* **83**(3) (2000) 461.
6. J. J. YU and I. W. BOYD, *Appl. Surf. Sci.* **208** (2003) 374.
7. A. V. CHADWICK, M. J POOLEY, K. E. RAMMUTLA, S. L. P. SAVIN and A. ROUGIER, *J. Phys. Cond. Matt.* **15** (2003) 431.
8. P. LI, I. W. CHEN, E. JAMES and J. E. P. HAHN, *Phys. Rev. B* **48** (1993) 10063.
9. DEBASIS BHOWMICK, D. NAIK, MD. EQBAL, D. SANYAL, S. DECHOUDHURY, V. BANERJEE, A. BANDYOPADHYAY, P. DEB, D. BHATTACHARYA and ALOK CHAKRABARTI, *Nucl. Instr. Meth. A* (in press); P. VAN DUPPEN, P. DECROCK, M. HUYSE, TH. DELBAR, W. GALSTER, P. LELEUX, I. LIENARD, P. LIPNIK, M. LOISELET, C. MICHOTTE, G. RYCKEWAERT, J. VERVIER, P. DUHAMEL and J. VANHORENBEECK, *Nucl. Instr. Meth. B* **70** (1992) 393.
10. E. T. KIM and S. G. YOON, *Thin Solid Films* **7** (1993) 227.
11. R. BIRRINGER, H. GLEITER, H. P. KLEIN and P. MARQUARDT, *Phys. Lett. A* **102** (1984) 356.
12. R. PASCUAL, M. SAYER, C. V. R. V. KUMAR and L. ZOU, *J. Appl. Phys.* **70** (1991) 2348.
13. H. HAHN, *Nanostruct. Mater.* **9** (1997) 3.
14. X. BOKHIMI, A. MORALES, M. PORTILLA and A. GRACIA-RUIZ, *ibid.* **12** (1999) 589.
15. W. G. LUO, A. L. DING and H. LI, *Integr. Ferroelectr.* **9** (1995) 75.
16. D. MICHEL, E. GAFFET and P. BERTHET, *Nanostruct. Mater.* **6** (1995) 667.
17. S. INDRIS, D. BORK and P. HEITJANS, *J. Mater. Synth. Process* **8** (2000) 245.
18. B. Q. ZHASNG, L. LU and M. O. LAI, *Physica B* **325** (2003) 120.
19. P. HAUTOJARVI and C. CORBEL, in "Positron Spectroscopy of Solids," edited by A. Dupasquier, A. P. Mills jr. (IOS Press, Ohmsha, Amsterdam, 1995), p. 491, in "Positron Annihilation in Semiconductors," edited by R. Krause-Rehberg and H. S. Leipner (Springer Verlag, Berlin, 1999).
20. B. E. WAREN, in "X-ray Diffraction" (Addison-Wesley, Reading, MA, 1969) p. 26419.
21. D. SANYAL, D. BANERJEE and UDAYAN DE, *Phys. Rev. B* **58** (1998) 15226.
22. P. KIRKEGAARD, N. J. PEDERSEN and M. ELDRUP, Report of Riso National Lab (Riso-M- 2740) 1989.
23. K. G. LYNN and A. N. GOLAND, *Solid State Commun.* **18** (1976) 1549.
24. R. S. BRUSA, W. DENG, G. P. KARWASZ and A. ZECCA, *Nucl. Instru. Meth. B* **194** (2002) 519.
25. V. J. GHOSH, M. ALATALO, P. ASOKA-KUMAR, B. NIELSEN, K. G. LYNN, A. C. KRUSEMAN and P. E. NIJNARENDS, *Phys. Rev. B* **61** (2000) 10092.
26. MAHUYA CHAKRABARTI, A. SARKAR, D. SANYAL, G. P. KARWASZ and A. ZECCA, *Phys. Letts. A* **321** (2004) 376.

Received 7 October 2004
and accepted 28 February 2005